Send Orders of Reprints at reprints@benthamscience.org

4534 *Current Medicinal Chemistry,* **2012**, *19,* 4534-4540

Alkyl Hydroxybenzoic Acid Derivatives that Inhibit HIV-1 Protease Dimerization

O.A. Flausino Jr.[a,b], L. Dufau[a], L.O. Regasini[b], M.S. Petrônio[b], D.H.S. Silva[b], T. Rose[c], V.S. Bolzani[b,*] and M. Reboud-Ravaux[a,*]

[a]*Enzymologie Moléculaire et Fonctionnelle, UR4, UPMC-Sorbonne Universités, 7 Quai St Bernard, 75252 Paris Cedex 05, France;* [b]*Chemistry Institute, Sao Paulo State University, CEP 14800-060, SP, Brazil;* [c]*Institut Pasteur, Unité d'Immunogénétique Cellulaire, 25 rue du Dr Roux, 75724 Paris Cedex 15, France*

Abstract: The therapeutic potential of gallic acid and its derivatives as anti-cancer, antimicrobial and antiviral agents is well known. We have examined the mechanism by which natural gallic acid and newly synthesized gallic acid alkyl esters and related protocatechuic acid alkyl esters inhibit HIV-1 protease to compare the influence of the aromatic ring substitutions on inhibition. We used Zhang-Poorman's kinetic analysis and fluorescent probe binding to demonstrate that several gallic and protecatechuic acid alkyl esters inhibited HIV-1 protease by preventing the dimerization of this obligate homodimeric aspartic protease rather than targeting the active site. The tri-hydroxy substituted benzoic moiety in gallates was more favorable than the di-substituted one in protocatechuates. In both series, the type of inhibition, its mechanism and the inhibitory efficiency dramatically depended on the length of the alkyl chain: no inhibition with alkyl chains less than 8 carbon atoms long. Molecular dynamics simulations corroborated the kinetic data and propose that gallic esters are intercalated between the two *N*- and *C*-monomer ends. They complete the β-sheet and disrupt the dimeric enzyme. The best gallic ester (14 carbon atoms, K_{id} of 320 nM) also inhibited the multi-mutated protease MDR-HM. These results will aid the rational design of future generations of non-peptide inhibitors of HIV-1 protease dimerization that inhibit multi-mutated proteases. Finally, our work suggests the wide use of gallic and protocatechuic alkyl esters to dissociate intermolecular β-sheets involved in protein-protein interactions.

Keywords: dimerization inhibitors; gallic acid alkyl esters; HIV-1 protease inhibition; intermolecular β-sheet inhibitors; protocatechuic acid alkyl esters.

INTRODUCTION

The mature human immunodeficiency virus type 1 protease (HIV-PR) has proven to be a successful target for the development antiviral agents. Synthetic PR inhibitors are now included in highly active antiretroviral therapy (HAART). HIV-PR is responsible for processing of polyproteins Gag and Gag-Pol into the mature viral enzymes and structural proteins need to build the virus capsid. Several protease active site inhibitors of HIV-PR (PIs) have been developed, but cross-resistance to these PIs seriously limits the long-term treatment of AIDS patients. It is therefore essential to identify new classes of antiretroviral drugs that act via another mechanism of action and have few or no adverse effects.

HIV-PR is only active as a dimer since the oligomerization of two identical protease monomers is required for catalytic activity [1]. The dimer interface involves mainly the *β*-hairpin flaps, the aspartic protease triad residues (Asp^{25}-Gly^{27}) and *N* (residues 1-4)-terminal and *C* (residues 96-99)-terminal *β*-strands of the two monomers [2]. The antiparallel *β*-sheet formed by interdigitation of these *N*- and *C*-terminal monomer ends contributes close to three-fourths of the total Gibbs free energy of dimerization [3]. Moreover, its amino acid residues are highly conserved in most HIV-1 isolates, in some HIV-2 isolates, and in drug-resistant HIV-1 variants [4]. Since mutations involved in resistance to one or more clinical PIs lie within or outside the active site but rarely in the antiparallel *β*-sheet formed by the *N*- and *C*-terminal monomer ends, this region has been the target of efforts to develop new protease inhibitors, named as HIV-PR dimerization inhibitors (Fig. **1**). Several series of dimerization inhibitors targeting this *β*–sheet region have been developed by us or others, including *C*- and *N*-terminal mimetic peptides [5-7], lipopeptides [8-10], bicyclic guanidinium derivatives [11], and cross-linked peptides with flexible spacers [12, 13] and semi-rigid ones [14-17].

*Address correspondence to these authors: M.R.R. at the Enzymologie Moléculaire et Fonctionnelle, UR4, UPMC-Sorbonne Universités, 7 Quai St Bernard 75252 Paris Cedex 05, France; Tel: +33(0)144275078; Fax: +33(0)144275140; E-mail: michele.reboud@upmc.fr; V.S.B. V.S.B. at the Institute of Chemistry, Rua Prof. Francisco Degni, 55, Sao Paulo State University, CEP 14800-900, SP Brazil; Tel: +55-16-331-6660; Fax: +55-16-3322-2308; E-mail: bolzaniv@iq.unesp.br

Recent reports of the antiviral activities of gallic acid derivatives [18, 19] led us to look for new inhibitors of HIV-1 protease dimerization among these molecules. Gallic acid and its derivatives are among the most abundant phenolic antioxidants in wines and green tea [20] and their antioxidant, antibacterial, anti-inflammatory, antimutagenic, and chemopreventive properties have been well documented [18, 21-25]. Lauryl gallate (dodecyl gallate) inhibits the enzyme xanthine oxidase and the peroxidation of mitochondrial lipids induced by Fe^{III}-NADPH with an IC_{50} of 10 μg/mL [26]. The anti-HIV-1 activity *in vitro* of 50 μM gallic acid and alkyl gallates was tested by exposing peripheral blood mononuclear cells to a suspension of HIV-1 [19]. The inhibition of viral replication depended on the length of the gallate alkyl chain. Similarly, the inhibition of HIV-1 integrase by gallic acid and its alkyl derivatives was also influenced by the alkyl chain length [27].

A recent report on the ability of alkyl tripeptides to inhibit the dimerization of HIV-PR showed a similar dependence on the length of alkyl chain [10]. The alkyl chain length influenced both their mechanism of action (active-site or dimerization or mixed inhibition) and their inhibitory potency.

We have now examined the mechanism by which two series of hydroxybenzoic acid derivatives inhibit HIV-PR (Fig. **2**): gallic acid (**1a**) and 15 alkyl esters (**1b-p**), and protocatechuic acid (**2a**) and 14 alkyl esters (**2b-n**)**.** The protocatechuic series was chosen to compare the influence of aromatic ring substitution on the inhibition. The length of the linear alkyl chain varied from 1 to 14 (**1b-1n**) and 1 to 18 (**2b-2o**) carbon atoms. Two branched alkyl chains were introduced into compounds **1o** and **1p**. We used kinetic analysis, Zhang-Poorman's method, and a complementary assay, fluorescent probe binding using 8-anilino-1-naphtalene-sulfonic acid (ANS), to investigate the influence of the hydrophobic alkyl chain on the mechanism by which these new hydroxybenzoic acid derivatives inhibit HIV-PR. We demonstrated for the first time that several gallic and protocatechuic alkyl esters acted as dimerization inhibitors of HIV-PR. They also inhibited by the same mechanism the multi-mutated protease MDR-HM whom mutations are identical to that found in some resistant HIV strains. Finally, we checked out our experimental results with molecular dynamics simulations of the alkyl hydroxybenzoic acid derivatives complexed with wild-type and mutated HIV-PR monomers.

1875-533X/12 $58.00+.00

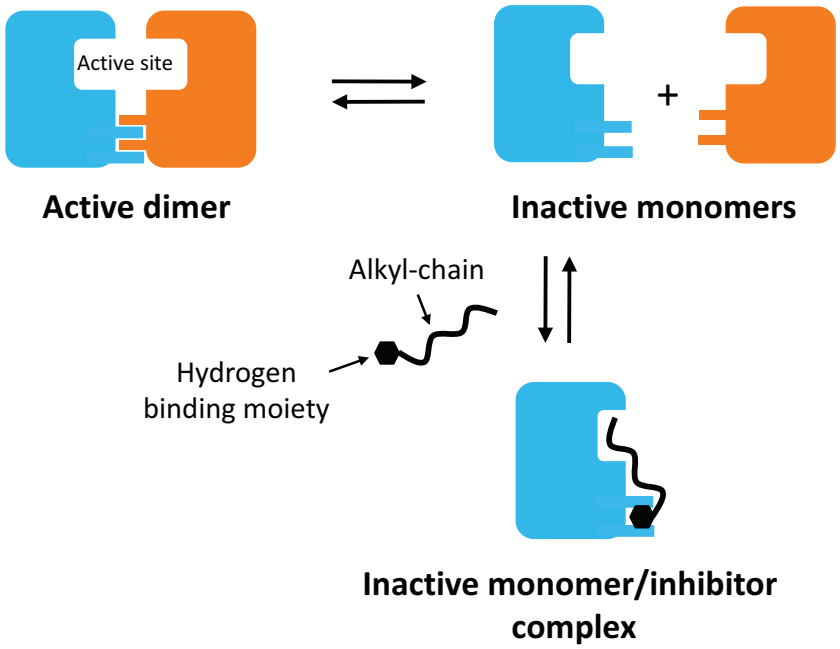

Fig. (1). Mechanism by which an alkyl dimerization inhibitor may act as a homodimer disruptor to inhibit HIV-1 PR.

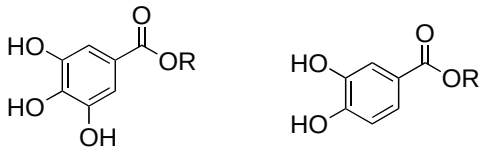

R		Series 1	R		Series 2
H		**1a**	H		**2a**
	n			n	
	0	**1b**		0	**2b**
	1	**1c**		1	**2c**
	2	**1d**		2	**2d**
	3	**1e**		3	**2e**
	4	**1f**		4	**2f**
	5	**1g**		5	**2g**
$-(CH_2)_n-CH_3$	6	**1h**	$R-(CH_2)_n-CH_3$	6	**2h**
	7	**1i**		7	**2i**
	8	**1j**		8	**2j**
	9	**1k**		9	**2k**
	10	**1l**		11	**2l**
	11	**1m**		13	**2m**
	13	**1n**		15	**2n**
				17	**2o**
	n				
$-(CH_2)_n-CH-(CH_3)_2$	0	**1o**			
	1	**1p**			

Fig. (2). Chemical structures of semi-synthetic derivatives **1** (gallates) and **2** (protocatechuates).

MATERIALS AND METHODS

1. Gallic Acid Source

Gallic acid was extracted from *Alchornea glandulosa*. The leaves were collected in the Biological Reserve and Experimental Station at Mogi Guaçu, SP, Brazil, in March 2005. A voucher specimen (SP319257) has been deposited in the herbarium of the Botanic Institute (São Paulo, SP, Brazil). The shade-dried plant material (1.5 kg) was ground and defatted with *n*-hexane (3.5 L x 3, at room temperature) and exhaustively extracted by maceration with MeOH (4.2 L x 3). The crude extract was concentrated under pressure to yield 3.8 g of a syrup residue. The concentrate was then diluted with MeOH/H_2O (4:1) and successively partitioned with EtOAc and *n*-BuOH. After solvent removal under reduced pressure, the partition phases yielded 2.5 and 0.8 g, respectively. The EtOAc residue (2.0 g) was chromatographed by gel permeation over Sephadex LH-20, eluted with methanol, to afford 11 fractions (A1-A11). Fraction A2 (730 mg) was further purified by reverse-phase (RP)-HPLC (7.5:92:0.5 MeOH/H_2O/HOAc, UV detection at 265 nm, and flow rate at 15 mM/min) to yield gallic acid (355 mg). The identification was based on analysis of its ^1H and ^{13}C NMR data, as well as by comparison to the chemical product obtained from Sigma-Aldrich Chemical Co. (St. Louis, MO).

2. Synthesis

2.1. Synthesis of Gallates and Protocatechuates

A 3.0 mL solution of *N*,*N*'-dicyclohexylcarbodiimide (DCC, 1.0 mmol) in dried *p*-dioxane was added to a cooled (5 ^oC) solution of 0.2 mmol of protocatechuic acid or gallic acid and 20 mmol of *n*-alkyl alcohol in 6.0 mL of dried *p*-dioxane. The solution was stirred for 48 h, and the solvent was subsequently removed under reduced pressure. The residue was partitioned with EtOAc (3 times) and filtered. The filtrate was washed successively with saturated aqueous citric acid solution (3 times), saturated aqueous $NaHCO_3$ (3 times), dried over anhydrous $MgSO_4$, and evaporated under reduced pressure. The crude products were purified over a silica gel column eluted with $CHCl_3$/MeOH (98:2) to afford alkyl esters. Structures of the semi-synthetic esters were established by ^1H and ^{13}C NMR spectral analysis.

2.2. Synthesis of Acylated Analogues

For synthesis of acylated analogues, protocatechuic acid or gallic acid (20 mmol) was dissolved in dried pyridine (5.0 mL) and acetic anhydride (5.0 mL) under hydrogen atmosphere. The mixture was stirred for 48 h at room temperature, dried under reduced pressure, and purified by column chromatography with $CHCl_3$/MeOH (85:15). Structures of the acylated analogues were established by ^1H and ^{13}C NMR spectral analysis.

3. Mutated Proteases

We produced a pseudo-wild type protease (called here PR) and the multi-mutated protease MDR-HM (L10I/M46I/ I54V/V82A/ I84V/L90M) as described in [10]. The monomer of PR had 5 mutations: Q7K, L33I, L63I to minimize protease autolysis, and C67A and C95A to prevent cysteine-thiol oxidation. The enzymatic activity of the pseudo-wild type protease containing these protective mutations was identical to that of wild-type protease. The plasmid pET9PRWT bearing the wild-type sequence of the protease gene from HIV (BRU) DNA clone (subclone of λJ19) was used as template for PCR amplification cycles. The resulting mutated plasmids were sequenced (Genome Express, Meylan, France) on both coding and noncoding strands. The PR and MDR-HM protease [28] (Prof. E. Freire, the Johns Hopkins University, Baltimore, MD) were expressed in *Escherichia coli* BL21 (DE3) rosetta pLysS strain (Novagen, Darmstadt, Germany), purified, and refolded as described before [10].

4. Enzyme and Inhibitor Assays

The fluorogenic substrate DABCYL-γ-abu-SQNYPIVQ-EDANS (DABCYL, 4-(4'-dimethylaminophenylazo)benzoyl; γ-abu, γ-aminobutyric acid; EDANS, 5[(2-aminoethyl) amino]naphthalene-1-sulfonic acid) was purchased from Bachem (Voisins-le-Bretonneux, France). 1-anilino-8-naphthalene sulfonate (ANS) and acetylpepstatin were from Sigma-Aldrich, saquinavir was from the NIH (USA). Fluorescence intensities were measured in a FluoStar Galaxy spectrophotometer (BMG LabTechnologies, Offenburg, Germany) in black opaque microplates (Costar, Corning Incorporated, Corning, NY, USA).

The proteolytic activities of mutated proteases were determined fluorometrically (λ_{ex} = 340 nm; λ_{em} = 490 nm) in 100 mM sodium acetate, 1 mM EDTA, and 1 M NaCl at pH 4.7 and 30°C. The substrate (5.2 μM) and the compounds were first dissolved in DMSO. The final DMSO concentration was kept at 3% (v/v). The mechanism of inhibition and the corresponding kinetic constants K_{ic} (competitive inhibition) and/or K_{id} (dimerization inhibition) were determined using [7]. Plots were fitted using KaleidaGraph 4.0 (Synergy Software). Six concentrations of PR and mutated HDR-HM protease ($[E]_0$ = 5.33 - 18.7 nM for PR, and 10-20 nM for MDR-HM protease) were used for Zhang-Poorman kinetic analysis. The inhibitor concentrations were 1.13 and 0.85 μM for **1n**, 1.42 and 1.13 μM for **1m**, 2.55 and 1.98 μM for **1l**, 5.67 and 3.54 μM for **1k**, 11.33 and 8.5 μM for **1j**, 85 and 20 μM for **2m**, 5.67 and 1.7 μM for **2l**, 28.3 and 14.2 μM for **2k**, 17 and 8.5 μM for **2j,** 85 and 28 μM for **2i**.

5. Fluorescent Binding Probe

The intensity of the 8-anilino-1-naphtalene-sulfonic acid (ANS) fluorescence (λ_{exc}= 340 nm; λ_{em}= 490 nm) was measured (Perkin Elmer LS50B spectrofluorometer) using six ANS concentrations varying from 0 to 60 μM (final volume 200 μL) in the presence of PR alone (0.27 nM) (blank), and PR plus inhibitors (1.0 μM) as described in [10]. The final DMSO concentration was always 0.2 % (v/v). Each fluorescence measurement was made five times and averaged. PR, acetylpepstatin, saquinavir and compounds **1n** and **1m** had negligible intrinsic fluorescence under our experimental conditions.

6. Molecular Modeling

The PR/inhibitor complexes were modeled in five steps, as detailed previously for PR/lipopeptides [10]. 1) We first built an PR/compound **2m** model from crystallographic data for the dimer (1AXA, resolution 2.0 Å; [29]), replacing the monomer B *C*-terminus with **2m**, then with compounds **1** (n = 9-13) or **2** (n = 9-16). 2) We then evaluated the flexibility of monomer A loops from restrained molecular dynamics (Discover, Accelrys, San Diego, CA) and selected normal modes [30] that might enhance compound binding and set up starting models for PR. 3). The docking of compounds was processed on the same starting models using the superimposition of the alkyl chain. 4) We ranked the models of the complex according to stereochemical and energy criteria and optimized the best model PR monomer/compound **1** and PR monomer /compound **2** for each value of n from 9 to 16. 5) We compared the binding energies of the two series of inhibitors to PR and multi-mutated MDR-HM.

RESULTS AND DISCUSSION

Initial screening assays showed that gallic acid (**1a**) and protocatechuic acid (**2a**) and their derivatives with linear chains shorter than 9 carbons did not inhibit PR, even at the highest inhibitor concentration tested (50 μM). We determined the mechanism of inhibition for the active compounds (**1j-1n** and **2j-2n**) using Zhang-

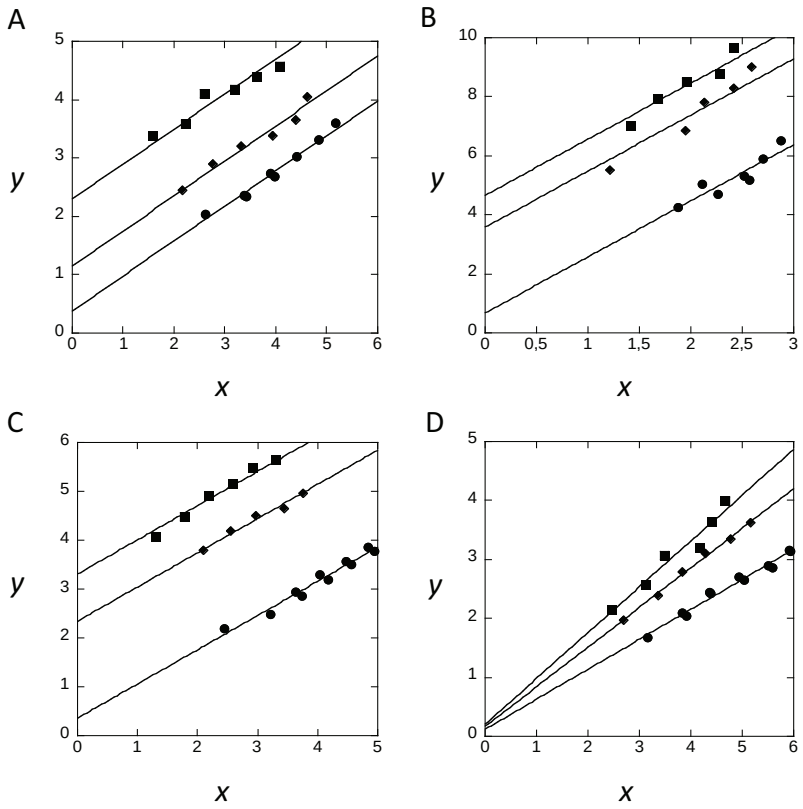

Fig. (3). Zhang-Poorman graphics for the inhibition of PR (A, C and D) and MDR-HM protease (B) by alkyl hydroxybenzoic acid derivatives at pH 4.7 and 30 °C. A. PR inhibition by **1n**: 1.13 μM (■), 0.85 μM (◆). B. MDR-HM protease inhibition by **1n**: 5.55 μM (■), 1.98 μM (◆). C. PR inhibition by **2m**: 5.6 μM (■), 1.7 μM (◆). D) PR inhibition by **1l**: 2.55 μM **4** (■), 1.98 μM (▲). Enzyme activity was also always measured without inhibitor (●).

x: $\sqrt{\text{vi}} \times 10^5 \left(\text{M}^{\frac{1}{2}}.\text{s}^{\frac{1}{2}} \right)$; y: $\frac{[E]_0}{\sqrt{\text{vi}}} \times 10^4 \left(\text{M}^{\frac{1}{2}}.\text{s}^{\frac{1}{2}} \right)$.

Poorman kinetic analysis [7]. Plots of $[E]_0/\sqrt{v_i}$ *vs* $\sqrt{v_i}$ were constructed to discriminate between inhibition of dimerization alone (parallel lines), competitive inhibition (altered slopes and unaltered *y*-axis intercepts), and mixed inhibition (altered slopes and altered *y*-axis intercepts) (Fig. **3**). The data for alkyl hydroxybenzoic derivatives showed that inhibitors with longer alkyl chains of 12 to 14 C (series **1**) and 12 to 16 C (series **2**) acted as pure dimerization inhibitors of PR. Gallic acid derivatives inhibited PR with inhibition constants (K_{id}) of 320 nM for **1n** (14 C) and 650 nM for **1m** (12 C) (Fig. **3**). The same mechanism also characterized the effects of **2n** (16 C), **2m** (14 C) and **2l** (12 C) with K_{id}s of 9.9, 0.5, and 2.1 μM, respectively (Fig. **3**). Compounds with shorter alkyl chains (9-11 carbons for series **1**, 9-10 for series **2**) acted as mixed inhibitors with an antidimer component characterized by a K_{id} value and a competitive component (binding within the active site) characterized by a K_{ic} value (Table **1**). The values of K_{id} and K_{ic} were almost identical in some cases, (**1l**, **1k, 2j**) while the dimerization process was preponderant in others (**1j**, **2k).** Branched alkyl chains were unfavorable (no inhibition at 50 μM for **1o** and **1p**).

We used direct structural investigation to examine further how alkyl hydroxybenzoic acid derivatives inhibit HIV proteases. The fluorescence emission for the binding of the fluorescent probe ANS was measured in the presence of two active site inhibitors (acetylpepstatin and saquinavir) and compounds **1m** and **1n** both identified as dimerization inhibitors. ANS is reported to preferentially attach to the hydrophobic zones of protein surfaces and binding leads to an increase in fluorescence. Adding ANS to a mixture of PR and compound **1n** increased the emission fluorescence (factor ≈ 2-times more than for PR plus ANS ([ANS] = 30 μM) (Fig. **4**). The same ANS concentration produced a smaller fluorescence increase with compound **1m** (≈ 1.6-fold). In contrast, the active site inhibitors saquinavir and acetylpepstatin decreased the fluorescence emission. These results suggest that compounds **1m** and **1n** were bound to unmasked hydrophobic surfaces of PR, in agreement with an inhibition of PR dimerization as this process is expected to expose hydrophobic interface areas due to dimer destabilization or dissociation [10, 15].

Gallic acid derivatives **1** had greater antidimer potential towards PR than did protecatechuic acid derivatives **2** with an identical alkyl chain. It was about 1.6-fold for C14 alkyl chains (**1n** and **2m**), 3.2-fold for C12 (**1m** and **2l**), 1.7-fold for C10 (**1k** and **2k**) and 11-fold for C9 (**1j** and **2k**). The same was true for mixed inhibitors (**1j** and **2j,** and **1k** and **2k**). The difference could be because gallic acid derivatives have three aromatic hydroxyl groups that can form hydrogen bonds, while protecatechuic acid derivatives have only two as evidenced below in modeled complexes.

Bannwarth and collaborators reported that the length of the alkyl chains greatly influenced the antidimer activity of alkyl tripeptides [10]. They showed that the lipotripeptides $CH_3(CH_2)_nCO$-YEL and $CH_3(CH_2)_nCO$-LEY with alkyl chain length of 12-16 carbons inhibited the dimerization of HIV-1 PR, whereas compounds with 8-10-carbon alkyl chains were mixed inhibitors. Lipopeptides with alkyl chains shorter than 6 carbons were pure competitive inhibitors. Our present results indicate that hydroxybenzoic acid derivatives with alkyl chains shorter than 7 carbons do not inhibit HIV-1 PR. The major difference between alkyl tripeptides and alkyl hydroxybenzoic acid derivatives resides is the nature of the moiety

Table 1. Inhibition of PR and Mutated HIV-1 Protease MDR-HM by Compounds 1 and 2 (30 °C and pH 4.7). [a]Standard Errors of Initial Rates are Less than 5%. NI: No Inhibition at 50 μM.

HIV-1 protease	Compounds		n	K_{id}[a] (μM)	K_{ic}[a] (μM)
	Gallic acid and derivatives				
PR	R = H	**1a**		NI	
	R = -$(CH_2)_n$-CH_3	**1b-1i**	0-7	NI	
		1j	8	2.5	31.5
		1k	9	7.9	12.3
		1l	10	3.9	5.5
		1m	11	0.65	
		1n	13	0.32	
	R = -$(CH_2)_n$-CH-$(CH_3)_2$	**1o**	0	NI	
		1p	1	NI	
	Protocatechuic acid and derivatives				
PR	R = H	**2a**		NI	
	R = -$(CH_2)_n$-CH_3	**2b-2i**	1-7	NI	
		2j	8	27.8	46.8
		2k	9	13.4	73.9
		2l	11	2.1	
		2m	13	0.5	
		2n	15	9.9	
		2o	17	NI	
MDR-HM		**1n**	13	0.69	

bearing the alkyl chain: it is a tripeptide in one case and a substituted benzoic acid in the other. This could lead to different interactions with the monomer *N*- and *C*-ends as suggested in PR/monomer inhibitor complexes.

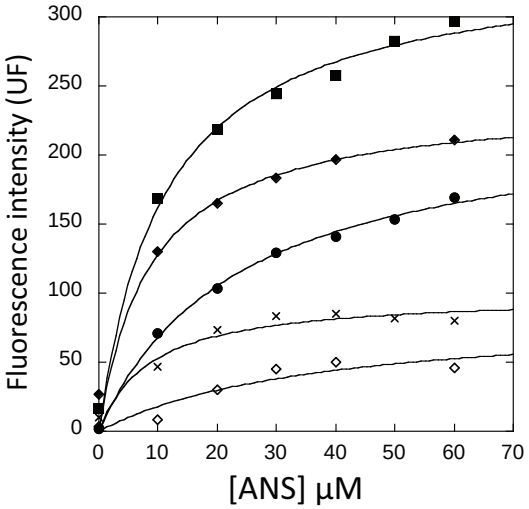

Fig. (4). ANS emission fluorescence (470 nm) measured at pH 4.7 and 25°C. The excitation wavelength was 370 nm. PR (275 nM) was preincubated without inhibitor (●) or with acetylpepstatin (◇), saquinavir (×) or compounds **1n** (■), **1m** (◆) prior to adding ANS. The inhibitor concentrations was 1 μM for all compounds. The final DMSO concentration was always 0.2 % (v/v). Fluorescence intensity was corrected for the fluorescence of the same concentrations of ANS and inhibitor in the absence of enzyme.

Models of PR monomer/inhibitor complexes corroborated the kinetics, with C14 alkyl chain providing an optimal occupancy of the hydrophobic enzyme cleft. In the model of the PR monomer/**2m** complex, the wide cleft in monomer A where the helix R^{B87}-G^{B93} of monomer B usually sits is narrowed by the closure of loops T^{A4}-P^{A9}, L^{A24}-D^{A30}, I^{A66}-K^{A70} and the β-hairpin flap M^{A46}-K^{A55} over the alkyl chain. The cleft grasps the ligand tightly, which buries several hydrophobic side chains from the cleft floor (L^{A24}, I^{A84}), the adjacent loops (I^{A47}, I^{A50}, I^{A54}, V^{A82}) and covering the catalytic residue D^{A25}. The flap opening measured by the distance CαD^{A25}-CαI^{A50} is much more closed over the cleft filled by gallate **1n** (10 Å) in this "super-closed" model, than in the closed crystallographic dimer (13 Å) as shown previously [10]. This flap also buries hydrophobic residues V^{A32}, V^{A56}, V^{A75} and L^{A76}. The side chains of W^{A6} and F^{A99} are also closer to each other, partially burying the alkyl chains (C1-C4) of **2m** and **1n**. The other side of the alkyl moiety (C1-C6) is protected from solvent by L^{A97} and by aromatic rings themselves. The protocatechuate and gallate aromatic rings sit in between the two *N*-term and *C*-term β-strands. For protocatechuate derivatives: the ester carbonyl forms an H-bond with the N98 amide, the H from *meta* hydroxyl group makes an H-bond with the T96 carbonyl, the *para* hydroxyl group O forms an H-bond with the T96 hydroxyl H and amide. For gallate derivatives: the ester carbonyl forms an H-bond with the N98 amide, O from a *meta* hydroxyl group makes an H-bond with the T96 and the I3 H amide. The H from the *meta* hydroxyl group is engaged in H-bond with P1 carbonyl. Gallate derivatives form H bonds with both ends of the skeleton, while protocatechuate derivatives form H bonds with the *C*-terminus only. The tight fit of the ligand in the cleft excludes most water molecules from around the hydrophobic residues of the PR active site, thus optimizing the interface area. The rims of the cleft close up the ligands. The interface surface areas were computed from differences between the water accessible surface area of free molecules

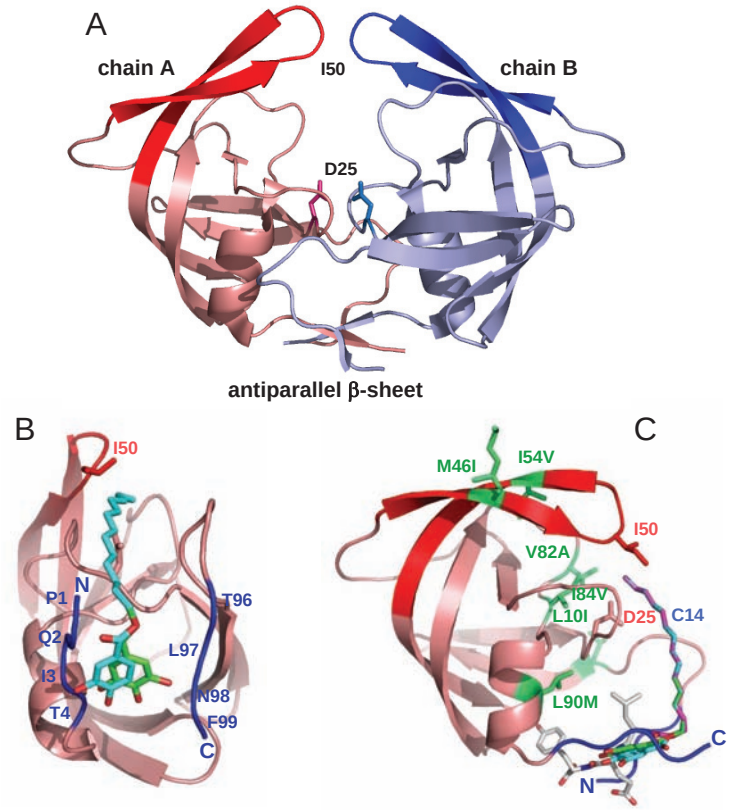

Fig. (5). Models of uncomplexed HIV-1 protease and complexes of C14 gallate **1n**, C14 catechuate **2m** and C14-LEY associated to a protease monomer (wild-type or MDR-HM). A. Open active site conformation of HIV-1 protease (ITW7, ligand-free dimer); chain A in red, chain B in blue. B. Models of monomer (red sketch) /**1n** (green sticks) and monomer (red sketch) /**2m** (turquoise sticks) complexes. *N*- and *C*- terminal monomer ends are in blue (green sticks) (90° rotation of the monomer from the front view A. The two alkyl chains of compounds **1n** and **2m** are perfectly superimposed. C. Models of compounds **1n** (green sticks) , **2m** (turquoise sticks) and C14-LEY (white sticks) associated to MDR-HM monomer showing a 'superclosed' protease conformation. Loops and flap motions improve the inhibitor binding. The closely superimposed alkyl chains do not interact with mutated side chains (mutations indicated in green). The tyrosine residue of C14-LEY occupies the" F99 pocket".

and the complex (probe radius = 1.4 Å). The PR interface with **2m**, $\Delta ASA_{PR/2m}$ = 616 Å^2, is composed of 14 % polar and 86 % nonpolar contributions. The PR interface with **1n** $\Delta ASA_{PR/1n}$ = 719 Å^2 is composed of 29 % polar and 71 % apolar contributions. The lipophilic alkyl chain is an important contributor to the interface (453 Å^2 for **1n** and 380 Å^2 for **2m**) and drive entropy of the free energy of inhibitor binding.

We also built protease-ligand models for alkyl chain lengths (n = 0-13) for the gallate series, n = 0-17 for the protocatechuate series and compared them with the previously reported alkyl tripeptide/monomer complexes [10]. The longest alkyl chains that could fit into the "super-closed" models were obtained for **1n** and **2m** displaying 14 carbon atoms whereas the best fit was observed with the palmitoyl moiety (16 carbon atoms) for lipopeptides. This agrees with the experimental results obtained for alkyl hydroxybenzoic acid derivatives, since compound **2n** (C16) acted as an antidimer whereas **2o** (C18) was not an inhibitor. The catalytic side chain D^{25} in the cleft is accessible to alkyl chains of C10 and longer ones (Fig. **5B**).

Finally, we measured the capacity of compound **1n**, which had the greatest inhibitory potential of all the compounds tested, to inhibit the multi-mutated protease MDR-HM. The MDR-HM variant has six mutations, two in the active site (V82A and I84V), two in the flap region (M46I and I54V) and two in the nearest dimerization region (L10I and L90M) [28]. Compound **1n** impaired the activity of MDR-HM by inhibiting the dimerization of the protease (K_{id} of 690 nM). The ratio $K_{id(MDR-HM)}/K_{id(PR)}$ was 2. The model of the complex formed between the PR monomer and **1n** suggests that the mutations in the monomer do not interfere with the inhibitor binding (Fig. **5C**).

All the above data indicate that the hydroxybenzoic acid derivatives are suitable new scaffolds on which to develop inhibitors of HIV-1 PR dimerization. They have the advantage to be non-peptide molecules that should be more stable and bioavailable *in vivo* than peptides. A weak toxicity of the gallic acid core and its alkyl derivatives has been reported [25,31]. The small size of the benzoic acid moiety indicates that they can be rationally optimized to increase the energy of binding to the *C*- and *N*-ends of the protease monomer by targeting the hydrophobic F99 pocket. Their unusual mechanism of action should enable them to circumvent the resistances due to treatments with active-site inhibitors PIs. They may also be good candidates for developing multi-target therapeutical agents in AIDS, since they may react with both the HIV-1 protease and its integrase [27], another pertinent target for AIDS treatment.

CONFLICT OF INTEREST

The author(s) confirm that this article content has no conflicts of interest.

ACKNOWLEDGEMENTS

We thank Prof. Ernesto Freire of the Department of Biology and Biocalorimetry Center, Johns Hopkins University, Baltimore,

MD, for the generous gift of the plasmid encoding the MDR-HM mutant. Saquinavir was obtained through the NIH AIDS Research and Reference Reagent Program, Division of AIDS, NIAID, NIH. The English text was edited by Dr Owen Parkes. We thank the French National Agency for Resaerch on AIDS and Viral Hepatitis for financial support (ANRS n°11359), CAPES (5329-09-4) and Sao Paulo State Research Funding Agency FAPESP for financial support (#03/02176-7 and #04/07932-7).

REFERENCES

[1] Wlodawer, A.; Miller, M.; Jaskolski, M.; Sathyanarayana, B.K.; Baldwin, E.; Weber, I.T.; Selk, L.M.; Clawson, L.; Schneider, J.; Kent, S.B., *Science,* **1989**, *245*, (4918), 616-621.

[2] Louis, J.M.; Weber, I.T.; Tozser, J.; Clore, G.M.; Gronenborn, A.M., *Adv Pharmacol,* **2000**, *49*, 111-146.

[3] Todd, M.J.; Semo, N.; Freire, E., *J Mol Biol,* **1998**, *283*, (2), 475-488.

[4] Hamacher, K., *Gene,* **2008,** *422*, (1-2), 30-36.

[5] Franciskovich, J., Houseman, K., Mueller, R., Chmielewski, J., *Bioorganic & Medicinal Chemistry Letters,* **1993**, *3*, (4), 765-768.

[6] Schramm, H.J.; Billich, A.; Jaeger, E.; Rucknagel, K.P.; Arnold, G.; Schramm, W., *Biochem Biophys Res Commun,* **1993**, *194*, (2), 595-600.

[7] Zhang, Z.Y.; Poorman, R.A.; Maggiora, L.L.; Heinrikson, R.L.; Kezdy, F.J., *J Biol Chem,* **1991**, *266*, (24), 15591-15594.

[8] Schramm, E.; Nowicky, J.W.; Godysh, Y., *Drugs under experimental and clinical research,* **1996**, *22*, (3-5), 247-254.

[9] Dumond, J.; Boggetto, N.; Schramm, H.J.; Schramm, W.; Takahashi, M.; Reboud-Ravaux, M., *Biochem Pharmacol,* **2003**, *65*, (7), 1097-1102.

[10] Bannwarth, L.; Rose, T.; Dufau, L.; Vanderesse, R.; Dumond, J.; Jamart-Gregoire, B.; Pannecouque, C.; De Clercq, E.; Reboud-Ravaux, M., *Biochemistry,* **2009**, *48*, (2), 379-387.

[11] Breccia, P.; Boggetto, N.; Perez-Fernandez, R.; Van Gool, M.; Takahashi, M.; Rene, L.; Prados, P.; Badet, B.; Reboud-Ravaux, M.; de Mendoza, J., *Journal of medicinal chemistry,* **2003**, *46*, (24), 5196-5207.

[12] Zutshi, R.; Chmielewski, J., *Bioorg Med Chem Lett,* **2000**, *10*, (17), 1901-1903.

[13] Ulysse, L.G.; Chmielewski, J., *Bioorg Med Chem Lett,* **1998**, *8*, (22), 3281-3286.

[14] Bouras, A.; Boggetto, N.; Benatalah, Z.; de Rosny, E.; Sicsic, S.; Reboud-Ravaux, M., *J Med Chem,* **1999**, *42*, (6), 957-962.

[15] Merabet, N.; Dumond, J.; Collinet, B.; Van Baelinghem, L.; Boggetto, N.; Ongeri, S.; Ressad, F.; Reboud-Ravaux, M.; Sicsic, S., *J Med Chem,* **2004**, *47*, (25), 6392-6400.

[16] Bannwarth, L.; Kessler, A.; Pethe, S.; Collinet, B.; Merabet, N.; Boggetto, N.; Sicsic, S.; Reboud-Ravaux, M.; Ongeri, S., *J Med Chem,* **2006**, *49*, (15), 4657-4664.

[17] Vidu, A.; Dufau, L.; Bannwarth, L.; Soulier, J.L.; Sicsic, S.; Piarulli, U.; Reboud-Ravaux, M.; Ongeri, S., *ChemMedChem,* **2010**, *5*, (11), 1899-1906.

[18] Ximenes, V.F.; Lopes, M.G.; Petronio, M.S.; Regasini, L.O.; Silva, D.H.; da Fonseca, L.M., *J Agric Food Chem,* **2010**, *58*, (9), 5355-5362.

[19] Kratz, J.M.; Andrighetti-Frohner, C.R.; Kolling, D.J.; Leal, P.C.; Cirne-Santos, C.C.; Yunes, R.A.; Nunes, R.J.; Trybala, E.; Bergstrom, T.; Frugulhetti, I.C.; Barardi, C.R.; Simoes, C.M., *Mem Inst Oswaldo Cruz,* **2008**, *103*, (5), 437-442.

[20] Paixao, N.; Pereira, V.; Marques, J.C.; Camara, J.S., *J Sep Sci,* **2008**, *31*, (12), 2189-2198.

[21] Kang, M.S.; Oh, J.S.; Kang, I.C.; Hong, S.J.; Choi, C.H., *J Microbiol,* **2008**, *46*, (6), 744-750.

[22] Kim, S.H.; Jun, C.D.; Suk, K.; Choi, B.J.; Lim, H.; Park, S.; Lee, S.H.; Shin, H.Y.; Kim, D.K.; Shin, T.Y., *Toxicol Sci,* **2006**, *91*, (1), 123-131.

[23] Birosova, L.; Mikulasova, M.; Vaverkova, S., *Biomed Pap Med Fac Univ Palacky Olomouc Czech Repub,* **2005**, *149*, (2), 489-491.

[24] Giftson, J.S.; Jayanthi, S.; Nalini, N., *Invest New Drugs,* **2010**, *28*, (3), 251-259.

[25] Morais, M.C.; Luqman, S.; Kondratyuk, T.P.; Petronio, M.S.; Regasini, L.O.; Silva, D.H.; Bolzani, V.S.; Soares, C.P.; Pezzuto, J.M., *Nat Prod Res,* **2010**, *24*, (18), 1758-1765.

[26] Kubo, I.; Masuoka, N.; Xiao, P.; Haraguchi, H., *J Agric Food Chem,* **2002**, *50*, (12), 3533-3539.

[27] Ahn, M.J.; Kim, C.Y.; Lee, J.S.; Kim, T.G.; Kim, S.H.; Lee, C.K.; Lee, B.B.; Shin, C.G.; Huh, H.; Kim, J., *Planta Med,* **2002**, *68*, (5), 457-459.

[28] Ohtaka, H.; Schon, A.; Freire, E., *Biochemistry,* **2003**, *42*, (46), 13659-13666.

[29] Spinelli, S.; Liu, Q.Z.; Alzari, P.M.; Hirel, P.H.; Poljak, R.J., *Biochimie,* **1991**, *73*, (11), 1391-1396.

[30] Lindahl, E.; Azuara, C.; Koehl, P.; Delarue, M., *Nucleic Acids Res,* **2006**, *34*, (Web Server issue), W52-56.

[31] Niho, N.; Tamura, T.; Toyoda, K., Uneyama, C., Takahashi, N.; Hirose, M., *Food and Chemical Toxicology*, **2001**, 39, 1063-1070.

Received: July 19, 2012 **Revised: August 14, 2012** **Accepted: August 26, 2012**